

Surface electronic structure of $\text{InSb}(\bar{1}\bar{1}\bar{1})3\times 3$ studied by angle-resolved photoelectron spectroscopy and scanning tunneling microscopy

L. Ö. Olsson, J. Kanski, and L. Ilver

Department of Physics, Chalmers University of Technology, S-412 96 Göteborg, Sweden

C. B. M. Andersson, M. Björkqvist, M. Göthelid, and U. O. Karlsson

Material Physics, Department of Physics, The Royal Institute of Technology, S-100 44 Stockholm, Sweden

M. C. Håkansson

Department of Synchrotron Radiation Research, University of Lund, S-223 62 Lund, Sweden

(Received 20 June 1994)

Valence-band spectra from the sputtered and annealed $\text{InSb}(\bar{1}\bar{1}\bar{1})3\times 3$ surface in normal emission and in the $\bar{\Gamma}\bar{M}$, $\bar{\Gamma}\bar{M}'$, and $\bar{\Gamma}\bar{K}$ azimuths have been measured. Some possible surface bands have been identified, among them one that clearly reflects the 3×3 periodicity of the surface. Core-level spectra of Sb $4d$ and In $4d$ were deconvoluted revealing one surface-shifted component for Sb $4d$ and, surprisingly, no pronounced surface-shifted component for In $4d$. Scanning tunneling microscopy images from this surface taken at different biases are presented. It is argued that the surface imaged at high bias is perturbed by the tip.

I. INTRODUCTION

With the perspective of continued device miniaturization, fundamental understanding of the electronic structure and atomic geometry at semiconductor surfaces becomes increasingly important. This, in combination with general interest in surface electron phenomena, motivates the large number of investigations devoted to semiconductor surfaces and interfaces. One universal feature of these surfaces is their ability to minimize the free energy by reconstructing. In some cases, the reconstructions are based on rather transparent principles, e.g., formation of dimers on (100)-type surfaces. Generally, however, the reconstructions are complicated, and despite considerable efforts on the theoretical as well as the experimental side, there are few cases of consensus concerning the surface characteristics. One cause for this is certainly the problem of well-defined surface preparation. For zinc-blende type crystals only the (110) surface can be obtained in a reasonably perfect state with good reproducibility, since it is produced by cleavage. Other preparation techniques, such as ion sputtering and annealing or molecular-beam epitaxy (MBE) give surfaces with different stoichiometries and, therefore, varying reconstructions. Although these surfaces can be classified by, e.g., low-energy electron diffraction (LEED), it is well known that similar LEED patterns can be obtained with different atomic arrangements. In some cases ambiguities concerning the geometry can be resolved by scanning tunneling microscopy (STM), but, as will be shown in this paper, this technique may also lead to ambiguity.

The situation is often improved if general trends can be found in data from similar systems. One such example is the family of $\{111\}$ surfaces of zinc-blende compounds. The anion-side ($\bar{1}\bar{1}\bar{1}$) surfaces of MBE-grown GaAs,

InAs, and InSb all show a 2×2 reconstruction, which is believed to be stabilized by anion trimers.¹⁻³ The cation-side (111) surfaces of GaAs, GaSb, GaP, and InSb also reconstruct as 2×2 , though in this case a vacancy buckling model is believed to describe the geometry.⁴⁻⁷ When prepared by ion sputtering and annealing the ($\bar{1}\bar{1}\bar{1}$) surfaces of GaAs,⁸ GaSb,⁸ and InSb (Ref. 9) show a 3×3 LEED pattern. This reconstruction has received less attention. Limited angle-resolved photoemission studies of $\text{InSb}(\bar{1}\bar{1}\bar{1})3\times 3$ in the $\bar{\Gamma}\bar{K}$ azimuth⁹ and normal emission¹⁰ have been reported. More recently, the $\text{InSb}(\bar{1}\bar{1}\bar{1})3\times 3$ surface was also studied by STM (Ref. 11) and x-ray diffraction.¹² Based on these data a model for the surface reconstruction involving complex adatom structures was proposed, in which, however, the 3×3 geometry is not transparent. In an attempt to get a more complete description of this surface we have carried out an extensive study of the surface electronic structure by means of angle-resolved photoelectron spectroscopy and also present STM data.

II. EXPERIMENT

The photoemission experiments were carried out in a VG ADES 400 system using rare-gas resonance lines (at Chalmers University of Technology) and in a modified VSW (Vacuum Science Workshop Ltd.) photoelectron spectrometer at the synchrotron radiation laboratory, MAX-lab in Lund. In both systems, the sample manipulators allowed for two rotations, around a vertical axis in the surface plane and around a horizontal axis co-linear with the surface normal. Both analyzers were movable in the plane of incidence (around a vertical axis) and at MAX-lab the analyzer could also be moved around a horizontal axis. The angular resolution was 2° and all data were recorded with 0.1-eV energy resolution. The

light incidence angle was kept constant at 45° . Spectra were recorded along the $\bar{\Gamma}\bar{M}$, $\bar{\Gamma}\bar{M}'$, and $\bar{\Gamma}\bar{K}$ azimuths in the surface Brillouin zone (SBZ) for emission angles between 0° and 80° and in a normal emission series with varying photon energy. The azimuthal orientation was varied by rotation of the sample itself and was controlled by LEED. The base pressure in the measurement chambers was $\sim 1\times 10^{-10}$ Torr.

The STM work was performed with a commercial Omicron instrument (at the Royal Institute of Technology) in an ultrahigh vacuum system with a base pressure of $\sim 3\times 10^{-11}$ Torr. Surface preparation and initial LEED analysis was performed in a separate vacuum chamber connected with the STM. Images were acquired with tungsten tips, electrochemically etched from a 0.25-mm wire in a NaOH solution under dc bias conditions.

The sample material was taken from a *p*-doped InSb(111) wafer (MCP Electronic Materials, Ltd.). The surfaces were cleaned by repeated cycles of 500-eV Ar^+ sputtering and annealing until a LEED pattern with sharp fractional order spots and low background was obtained.

III. RESULTS AND ANALYSIS

A. Valence band

A series of valence-band spectra with varying emission angles were measured for a few photon energies. In Fig. 1, spectra taken with 21.2-eV photon energy for the $\bar{\Gamma}\bar{M}$, $\bar{\Gamma}\bar{M}'$, and $\bar{\Gamma}\bar{K}$ azimuths are presented. The positions of all peaks and shoulders were determined by taking the second derivative of the spectra and were plotted as a function of k_{\parallel} in a "structure plot." The momentum parallel to the surface is conserved upon emission of an electron and is given by $k_{\parallel}(\text{\AA}^{-1})=0.512\sqrt{E_{\text{kin}}(\text{eV})}\sin\Theta$. To distinguish surface induced states from bulk contribution the direct bulk interband transitions were first identified by using a theoretical structure plot. In the calculations the initial bands were obtained using an empirical linear combination of atomic orbitals (LCAO) formalism¹³ and the final bands approximated by parabolic free-electron bands in an inner potential of 7 eV below the valence-band maximum (VBM). This approach also

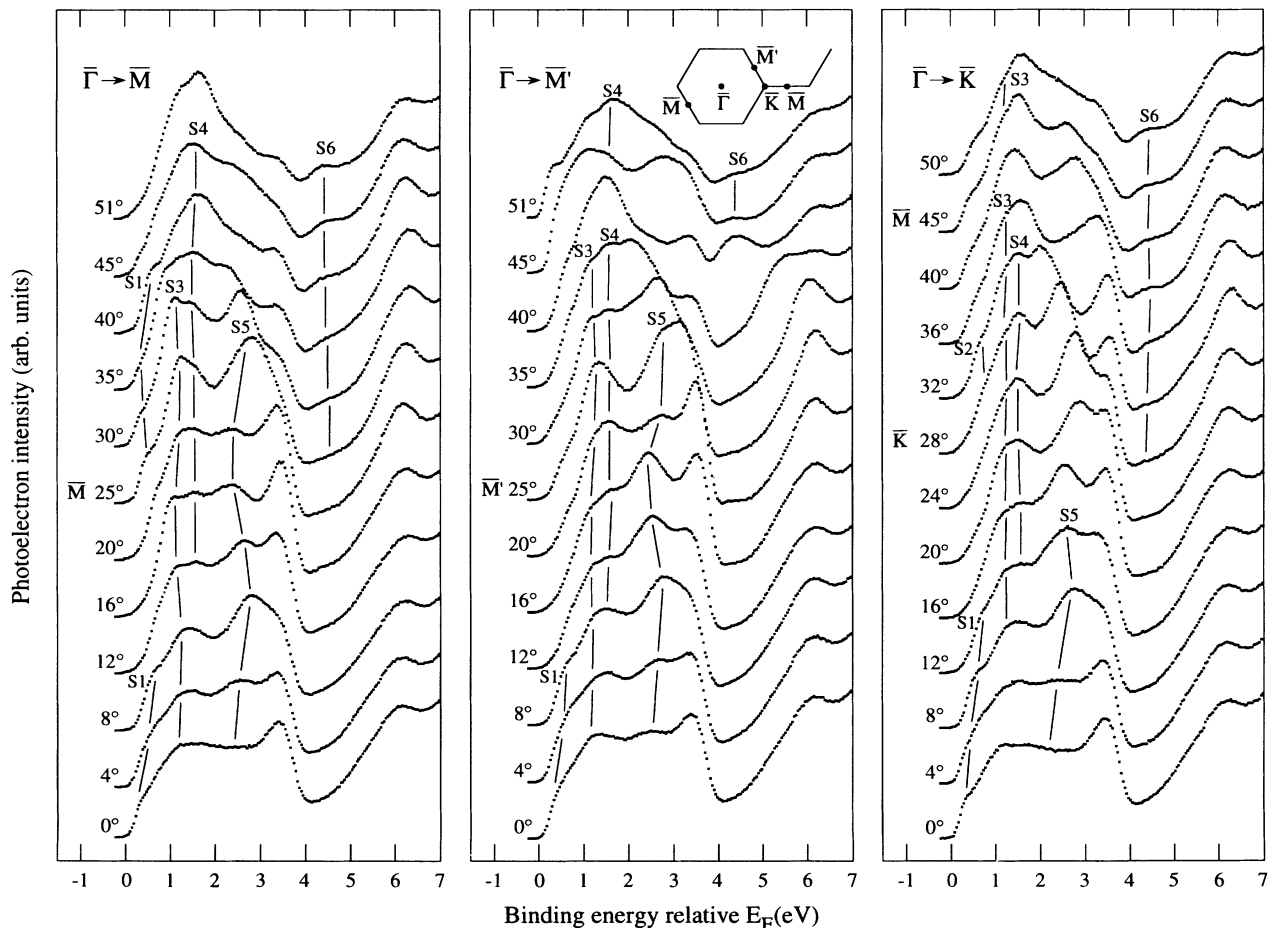


FIG. 1. Valence-band photoemission spectra obtained with 21.2-eV photon energy for different emission angles along the azimuths $\bar{\Gamma}\bar{M}$, $\bar{\Gamma}\bar{M}'$, and $\bar{\Gamma}\bar{K}$. The positions in spectra of symmetry points of the 1×1 SBZ are indicated next to the emission angles. Included is also the geometry of the SBZ.

made it possible to distinguish between the inequivalent $\bar{\Gamma}\bar{M}$ and $\bar{\Gamma}\bar{M}'$ azimuths, which corresponds to the “backbond” and “counterbackbond” directions, respectively. Apart from the bulk interband transitions also features at ~ 3.4 and ~ 6.1 eV are ascribed to bulk states, since they are interpreted as emission from high initial density-of-states regions (DOS) at Σ_{\min} and the bottom of the third band. The remaining peaks are shown in a structure plot in Fig. 2. Different symbols are used for different photon energies, with open symbols indicating weak features. The notations $S1$ – $S6$ are the same as those used in Fig. 1. The hatched area is the surface projection of bulk bands as calculated with the LCAO scheme. To get the calculated bulk bands on the same absolute energy scale as the experimental data, the position of the VBM relative to the Fermi level was determined by combining the binding energy of the bulk component of the In $4d$ core-level spectrum with the In $4d$ -VBM separation given by Taniguchi *et al.*¹⁴ With our value for the In $4d_{5/2}$ energy of 17.22 ± 0.05 eV relative to the Fermi level and the reported In $4d_{5/2}$ –VBM separation of 17.20 eV, we conclude that the VBM in our case is positioned very close to the Fermi level. This is in agreement with results reported by Höchst and Hernandez-Calderon.¹⁵

To test if the remaining peaks are surface induced, two criteria were used: (a) the peak positions in an E vs k_{\parallel} plot must be independent of photon energy and (b) they should show the periodicity of the SBZ. Also useful in the analysis is the fact that due to time-reversal invariance the $\bar{\Gamma}\bar{M}$ and $\bar{\Gamma}\bar{M}'$ azimuths are equivalent for surface bands, but not for bulk interband transitions. At this point a problem arises since emission from regions of

high initial DOS may be difficult to distinguish from surface bands. Just as for surface bands the positions of these features will be independent of photon energy and because of the small size of the reconstructed SBZ we expect the 3×3 dispersion of surface bands to be difficult to resolve. To some extent the surface projection of bulk bands will allow us to distinguish surface bands from DOS effects, since there are areas in a structure plot totally free from bulk bands. However, peaks appearing in a gap cannot automatically be identified as surface related on a reconstructed surface without considering the possibility of bulk transitions which are diffracted by the surface into the gap, i.e., surface umklapp.

Within 1.3-eV binding energy from the Fermi level all peaks are presented, except those identified as bulk interband transitions. In this range, there appear to be three surface induced structures, denoted $S1$, $S2$, and $S3$. Their dispersions are difficult to quantify. In the $\bar{\Gamma}\bar{M}'$ azimuth direct bulk interband transitions coincide with the expected positions of $S1$ and $S2$, and in all three azimuths these states have only appreciable intensity over limited parts of the SBZ. Further, $S1$ and $S3$ seem to overlap with a feature having 1×1 symmetry, which follows the edge of the projected bulk bands and has no dispersion with k_{\perp} . This is particularly apparent in the $\bar{\Gamma}\bar{M}$ azimuth where it might seem natural to join the data points by a band ranging from 0.3 eV at $\bar{\Gamma}_{1 \times 1}$ to 1.2 eV at $\bar{M}_{1 \times 1}$. A similar situation, with a weak feature following the edge of the projected bulk bands, is also found on InSb(111) 2×2 and InSb($\bar{1}\bar{1}\bar{1}$) 2×2 .¹⁶ Since a surface band should have the symmetry of the reconstructed surface, this would suggest that near the edge there is a contribution to spectra from regions of high DOS. The

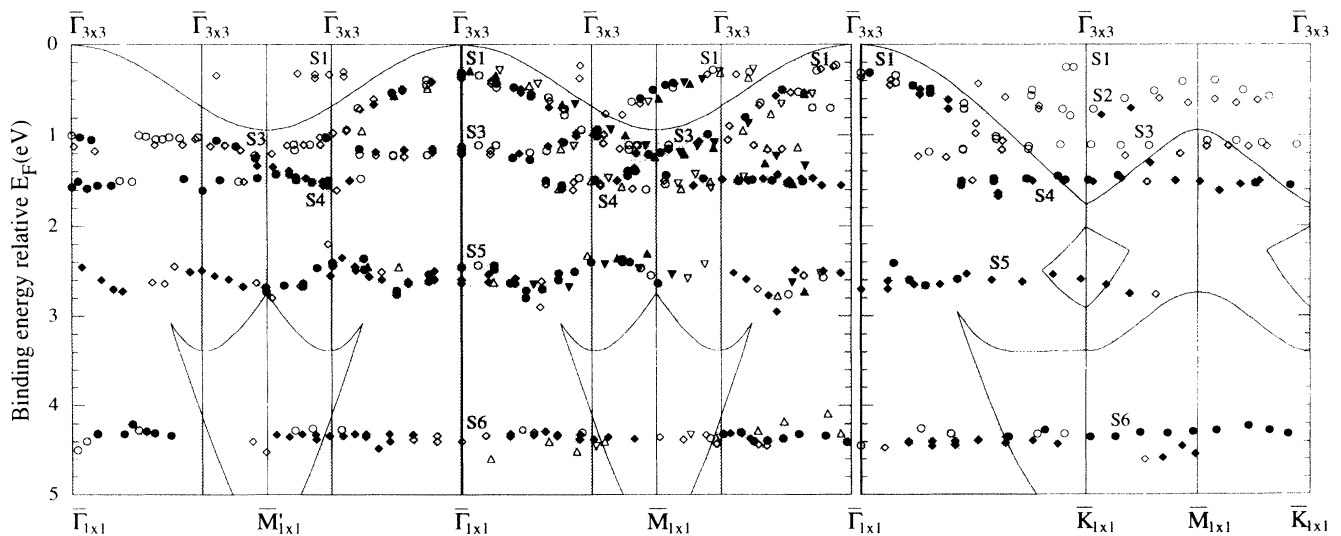


FIG. 2. Structure plot of spectral features that are candidates for being surface induced, obtained at 16.8 eV (\diamond), 20.0 eV (\triangle), 21.2 eV (\circ), and 24.0 eV (∇). Filled symbols represent well-defined structures while open symbols refer to weaker structures. The shaded area is the surface projection of bulk bands. The symmetry points of the 1×1 SBZ and the zone centers of the reconstructed 3×3 SBZ is given, with $\bar{\Gamma}$ corresponding to normal emission marked by a heavy line. The $S1$ and $S3$ surface bands are tentatively indicated by lines in regions where DOS structures interfere.

bandwidth (w) and dispersion of this feature is, however, different on $\text{InSb}(\bar{1}\bar{1}\bar{1})3\times3$ ($w\sim 0.9$ eV) than for the corresponding structures on $\text{InSb}(111)2\times2$ and $\text{InSb}(\bar{1}\bar{1}\bar{1})2\times2$ ($w\sim 1.2$ eV). Furthermore, in the $\bar{\Gamma}\bar{M}$ azimuth $S1$ appears in the gap of the projected bulk bands as a marked shoulder (see Figs. 1 and 3) while on $\text{InSb}(111)2\times2$ and $\text{InSb}(\bar{1}\bar{1}\bar{1})2\times2$ surfaces there are only very weak structures in this gap. Our conclusion is that the surface resonances $S1$ and $S3$ overlap with contribution from regions of high DOS near the edge of the projected bulk bands. To determine the dispersion of $S1$ in the $\bar{\Gamma}\bar{M}$ azimuth, peaks located in the bulk band gap are used, since here the contribution from overlapping DOS effects should be small. Such effects can only enter via surface umklapp processes, which are generally weak as is seen on $\text{InSb}(111)2\times2$ and $\text{InSb}(\bar{1}\bar{1}\bar{1})2\times2$.¹⁶ The location of $S1$ at $\bar{K}_{3\times3}$ is less certain since in the $\bar{\Gamma}\bar{K}$ azimuth $S1$ is only identified near the normal direction, where it overlaps with the projected bulk bands. This gives a dispersion of $S1$ from 0.3 eV at $\bar{\Gamma}_{3\times3}$ down to 0.5 eV at $\bar{M}_{3\times3}$, and at $\bar{K}_{3\times3}$ the binding energy is ~ 0.6 eV. The surface band $S3$ is located at ~ 1.2 eV and appears to disperse downwards from $\bar{\Gamma}_{3\times3}$. In the $\bar{\Gamma}\bar{K}$ azimuth $S3$ is seen only as a shoulder, but near the 1×1 zone boundaries in the $\bar{\Gamma}\bar{M}$ and $\bar{\Gamma}\bar{M}'$ azimuths it is one of the dominant peaks. This can be seen in Fig. 3, where spectra near $\bar{M}_{1\times1}$ are shown for different photon energies and measured along the three azimuths $\bar{\Gamma}\bar{M}$, $\bar{\Gamma}\bar{M}'$, and $\bar{\Gamma}\bar{K}$. The azimuthal dependency of the intensity supports the assignment, since DOS effects would be expected to appear with similar strength at equivalent points. The feature $S2$ was only seen in the bulk band gap near the second $\bar{\Gamma}_{3\times3}$ at 0.8 eV in the $\bar{\Gamma}\bar{K}$ azimuth. It is a marked shoulder in the 16.8-eV spectra (see Fig. 4). We cannot find any alternative obvious explanation of this

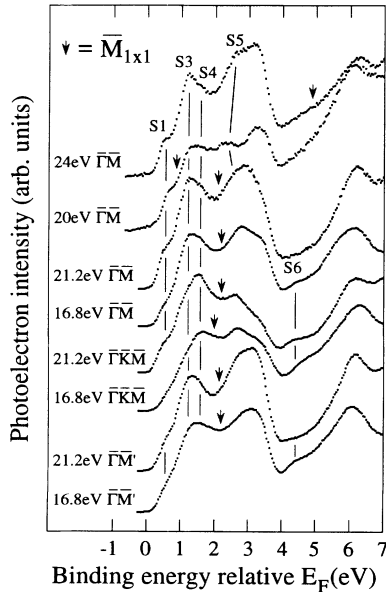


FIG. 3. Spectra taken near the equivalent point $\bar{M}_{1\times1}$ in the $\bar{\Gamma}\bar{M}$, $\bar{\Gamma}\bar{M}'$, and $\bar{\Gamma}\bar{K}$ azimuths with different photon energies. Arrows mark the exact position of $\bar{M}_{1\times1}$ in spectra.

structure in terms of surface umklapp of a bulk excitation in the plane of analysis. Away from $\bar{\Gamma}_{3\times3}$, $S2$ disperses upwards but its location at $\bar{K}_{3\times3}$ and $\bar{M}_{3\times3}$ is unclear. In the $\bar{\Gamma}\bar{M}$ and $\bar{\Gamma}\bar{M}'$ azimuths $S2$ is not seen at any $\bar{\Gamma}_{3\times3}$.

At larger binding energies three probable surface bands $S4$, $S5$, and $S6$ are recognized. The bands $S4$ at 1.5-eV and $S6$ at 4.3-eV binding energy have no resolvable dispersion. When determining the origin of $S4$ we must consider that the high DOS regime at the bottom of the second band coincides in energy. In Fig. 4, spectra with $S4$ in the vicinity of $\bar{K}_{1\times1}$ and $\bar{M}_{1\times1}$ are shown together with equivalent spectra from $\text{InSb}(111)2\times2$. Near $\bar{K}_{1\times1}$ $S4$ is a large peak where there is a gap in the projection of bulk bands (see Fig. 2) and there is no corresponding peak in spectra from the (111) surface. Further, at $\bar{M}_{1\times1}$ an edge in the (111) spectra is to be compared to the clear peak $S4$ on $(\bar{1}\bar{1}\bar{1})$. The fact that $S4$ appears in a gap at $\bar{K}_{1\times1}$ (i.e., $\bar{\Gamma}_{3\times3}$) is alone not proof that it reflects a surface band, since there are bulk bands at this energy displaced a surface reciprocal vector both at $\bar{\Gamma}_{1\times1}$ and at the second and third $\bar{\Gamma}_{3\times3}$ in the $\bar{\Gamma}\bar{M}$ and $\bar{\Gamma}\bar{M}'$ azimuths. The relatively high intensity of $S4$ in the gap and the comparison with spectra from the (111) surface justify, however, the assignment of $S4$ as a surface induced structure. The surface band $S6$ is seen at 4.3 eV over the whole SBZ and for all photon energies used, with no coinciding points with high initial bulk DOS. Although this state passes through the open lens of the projected bulk band structure (see Fig. 2) it does not imply that it is

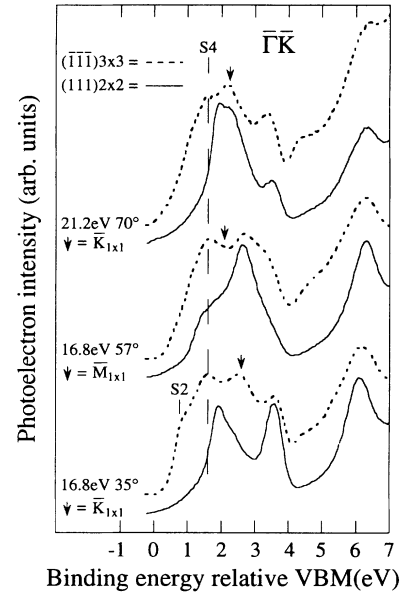


FIG. 4. Comparison of spectra from $\text{InSb}(\bar{1}\bar{1}\bar{1})3\times3$ and $\text{InSb}(111)2\times2$ taken along the $\bar{\Gamma}\bar{K}$ azimuth in the vicinity of the first $\bar{K}_{1\times1}$, $\bar{M}_{1\times1}$, and the second $\bar{K}_{1\times1}$. Arrows mark the exact position of these critical points in spectra. The position of the VBM relative the Fermi level is determined from the binding energy of the bulk component in $\text{In } 4d$ core-level spectra. The difference in pinning between the surfaces was (0.10 ± 0.05) eV with the Fermi level of $\text{InSb}(\bar{1}\bar{1}\bar{1})3\times3$ pinned closer to the VBM.

a “true” surface state (i.e., in contrast to a surface resonance), since in the reduced 3×3 zone scheme bulk states are folded into the gap region. This is also the case for the other surface bands considered, even though over some parts of the SBZ they appear in gaps of the unfolded bulk band projection. In the $\bar{\Gamma}\bar{M}$ and $\bar{\Gamma}\bar{M}'$ azimuths the surface band $S5$ clearly reflects the threefold periodicity of the surface. It disperses from 2.4 eV at $\bar{\Gamma}_{3 \times 3}$ down to 2.7 eV at $\bar{M}_{3 \times 3}$ and is located at ~ 2.7 eV at $\bar{K}_{3 \times 3}$.

Normal emission spectra obtained with photon energies between 17 and 46 eV are similar to the 0° spectra in Fig. 1 and, therefore, not shown here. We find that most features have no dispersion with k_\perp . As in off normal spectra, Σ_{\min} and the bottom of the third band are seen for most photon energies as a result of nondirect transitions. Also emission at the energies of the $S1$ and $S3$ surface bands is detected over the whole photon energy range. Above 40-eV photon energy a peak at 0.8 eV is seen, which could be emission from $S2$, and above 35 eV a broad feature, not previously mentioned, is found at ~ 5.1 -eV binding energy. At binding energies where we expect to find $S4$, $S5$, and $S6$ only weak peaks are detected for some photon energies.

It is instructive to compare the present data with those from relaxed anion terminated surfaces, such as InAs($\bar{1}\bar{1}\bar{1}$) 1×1 (Ref. 17) and InP($\bar{1}\bar{1}\bar{1}$) 1×1 .¹⁸ In these cases a surface band dispersing downwards from $\bar{\Gamma}$ near the VBM gives the dominant peak in spectra near normal emission. In band-structure calculations of these surfaces^{18,19} this peak is found to reflect the anion dangling-bond derived surface band. Since $S1$ has qualitatively a similar behavior, it is natural to assume that it derives from Sb dangling bonds. Further, we believe that the InSb($\bar{1}\bar{1}\bar{1}$) 3×3 surface contains less Sb dangling bonds than the 1×1 surface, since the dangling-bond density is generally reduced by reconstruction. This could then explain why this state has less intensity and smaller bandwidth than what is found on ($\bar{1}\bar{1}\bar{1}$) 1×1 surfaces. It is also worthwhile to note that a surface state at the same energy as $S6$ is also seen on InAs($\bar{1}\bar{1}\bar{1}$) 1×1 , dispersing through the gap of the bulk band projection. If not coincidental, this would mean that this state is not related to the outermost reconstructed layer but rather from beneath lying layers only subject to relaxation. This state was not reproduced in calculations of relaxed ($\bar{1}\bar{1}\bar{1}$) 1×1 surfaces.¹⁹

B. Core levels

The In $4d$ and Sb $4d$ core levels excited with 105-eV photons and observed in normal emission are presented in Fig. 5, together with fits to the data. In the fitting procedure the Lorentzian width was kept fixed and an integrated background was used. The bulk components were identified by imposing the established separation between the In $4d$ and Sb $4d$ levels¹⁴ and by observing shape changes with varying emission angles and kinetic energies. The Sb $4d$ core level shows one shifted surface component, while the In $4d$ core level is fitted with one dominant component. The latter fit is somewhat improved

when a small additional component is introduced. The intensity of this component increases with increasing surface sensitivity. Due to its very small amplitude, we believe that this structure is not a real feature of the 3×3 reconstruction, but is rather induced by some kind of surface defects. However, we do not exclude that it is an artefact of the fitting procedure, e.g., caused by an improper background function.

In the above-mentioned structure model, the 3×3 reconstruction is characterized by elliptic adatom rings oriented in three different azimuthal directions, on top of a complete InSb double layer.^{11,12} Within this model, which is partially derived from STM images similar to the high bias image shown in Fig. 6(a), each surface unit contains four In and two Sb atoms. One should thus expect to find a pronounced surface component in the In $4d$ spectrum. The preparation method would also imply a nonideal surface composition, i.e., both In and Sb atoms in the outermost layer. But, as already mentioned we do not observe any such component. Therefore, the presence of In atoms at the surface can only be reconciled with our data if it is assumed that all effects that contribute to surface shifts cancel each other (charge transfer,

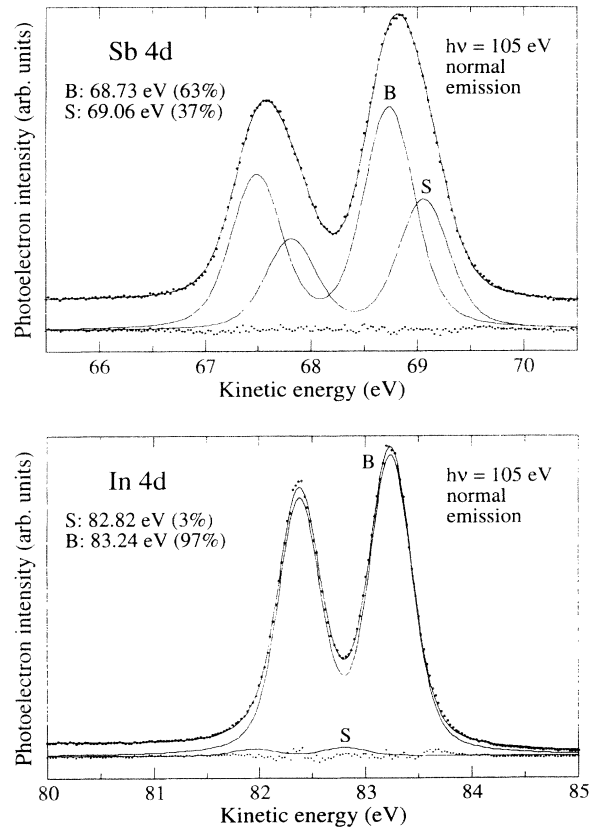


FIG. 5. Photoemission spectra of Sb $4d$ and In $4d$ core levels. Data points are presented together with fits to the data. Also shown is the decomposition into bulk (B) and surface (S) contributions and the residual. The shape parameters used for fitting the Sb $4d$ (In $4d$) core level are $\Delta E_{\text{Gauss}} = 0.44$ eV (0.37 eV), $\Delta E_{\text{Lor}} = 0.20$ eV (0.17 eV), $\Delta E_{\text{so}} = 1.25$ eV (0.86 eV), and branching ratio = 1.45 (1.18).

Madelung potential, final-state effects). Similar observations have been made for $\text{InSb}(111)2\times 2$ and $\text{InAs}(111)2\times 2$,²⁰ in which cases the anion core-level spectrum also contains only one component, although the vacancy buckling model for the geometry of these surfaces implies a change of the local surrounding of the surface anion atoms.

C. STM images

STM images of the reconstructed 3×3 surface are presented in Fig. 6(a) and 6(b). The images were acquired at a sample bias of -2.2 and -0.6 V, respectively, thus probing occupied electron states. The high bias image (a) displays two different types of surface units: one consisting of two high and two low protrusions, “ α type,” and one consisting of three protrusions of equal height, “ β type.” The α -type unit takes on three different orientations on the surface with equal probability and an angular rotation of 120° between them, while the β -type unit has two orientations, rotated 180° . The surface consists of 8–15% β while the remaining and dominant part is α -type units. In the low bias image (b) there are still two distinct surface units, distinguished in the image by rela-

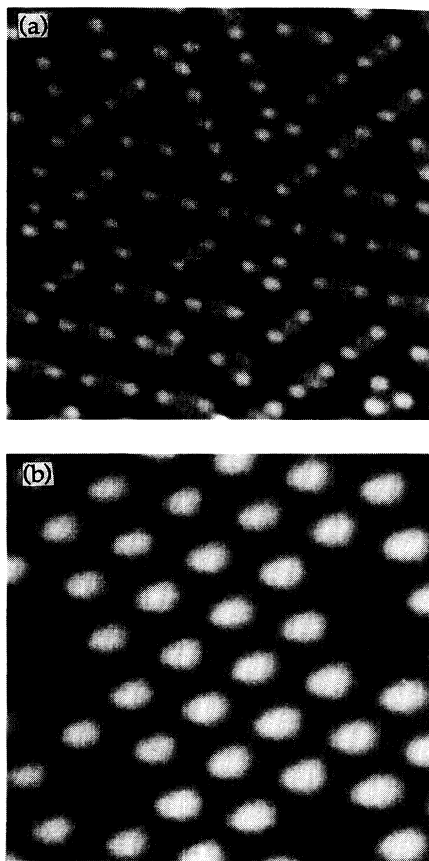


FIG. 6. STM images, $80\times 80 \text{ \AA}^2$, of the reconstructed 3×3 surface at a tunneling current of 1.4 nA and sample bias of -2.2 V (a) and -0.6 V (b). Two different surface units exist with the high bias image (a) revealing three (β) or four (α) protrusions per unit cell.

tive brightness. The relative occurrence of the two types of surface units in the low bias image is about the same as in the high bias image, which suggests that the dark units correspond to β -type surface units and the bright ones to α type. To tell anything about the structure within the two units in the low bias image is intricate, but both types appear to be triangular in shape and similarly oriented, in contrast to the high bias image.

The two types of images were usually not possible to obtain just by tuning the bias voltage. When going from low to high bias voltage, or *vice versa*, the other type of image could normally be obtained only after a change in the tip configuration. This indicates that the ability to probe the two different bias regimes is tip dependent. The reason for this is not clear, but it is possible that in one of the regimes the tip prefers to form an antimony or indium apex by adsorption from the surface. Once a certain type of image is obtained, the system is very stable and images reproducible.

The high bias image appears to be inconsistent with our valence-band data. The α -type surface unit is in majority and should, therefore, dominate the surface characteristics. It has twofold symmetry in the high bias image and is found with equal probability in three different orientations rotated by 120° . This would imply that the surface has not truly a 3×3 geometry, although LEED patterns as well as the surface band ($S5$) dispersion show that this is the case. It could perhaps be argued that if the scattering properties of the α -type unit are orientation independent in LEED, a 3×3 pattern could be obtained. However, we believe that the surface potential, which determines the dispersion of surface bands, is very sensitive to the detailed atomic configuration within the surface layer. Therefore, we conclude that the surface band $S5$ shows the true surface periodicity and that the surface is in some way perturbed when imaged at high voltage with STM. Indeed, the low bias image appears to show the 3×3 periodicity [see Fig. 6(b)]. Tip induced rearrangement of surface units at high bias has been reported previously.²¹ In the case of the $\text{InSb}(\bar{1}\bar{1}\bar{1})3\times 3$ surface it is interesting to note that Seehofer, Krivorotov, and Johnson report that the α units may appear rotated in different images from the same area taken with high bias.¹¹ No such effects were seen in this study but we suggest that this phenomenon is related with perturbations induced by high bias imaging.

IV. SUMMARY

Angle-resolved valence-band spectra from $\text{InSb}(\bar{1}\bar{1}\bar{1})3\times 3$ are found to be dominated by surface-state emission. The detailed analysis of the surface bands is partly obscured by overlapping DOS structures. In one case, however, a clear threefold periodicity is observed. The interpretation of the remaining structures is based on calculations of bulk interband transitions and comparison with photoemission from other $\text{InSb}\{111\}$ -type surfaces.

Core-level spectra reveal one pronounced surface-shifted Sb $4d$ component but no significant In $4d$ surface component. The lack of surface-shifted In states is found surprising, since considering the preparation technique,

we would expect In to be present at the surface.

STM images from this surface, taken at low and high biases of filled surface states, are quite different. The surface imaged at high bias is believed to be perturbed by the tip since the displayed surface geometry does not resemble a true 3×3 reconstruction.

ACKNOWLEDGMENTS

The expert technical assistance of the MAX-lab staff is gratefully acknowledged. This work was supported by grants from the Swedish Natural Science Research Council.

-
- ¹T. Nakada and T. Osaka, *Phys. Rev. Lett.* **67**, 2834 (1991).
²D. K. Biegelsen, R. D. Bringans, J. E. Northrup, and L.-E. Swartz, *Phys. Rev. Lett.* **65**, 452 (1990).
³C. B. M. Andersson, U. O. Karlsson, M. C. Håkansson, L. Ö. Olsson, L. Ilver, J. Kanski, and P. O. Nilsson (unpublished).
⁴S. Y. Tong, G. Xu, and W. N. Mei, *Phys. Rev. Lett.* **52**, 1693 (1984).
⁵R. Feidenhans'l, M. Nielsen, F. Grey, R. L. Johnson, and I. K. Robinson, *Surf. Sci.* **186**, 499 (1987).
⁶G. Xu, W. Y. Hu, M. W. Puga, S. Y. Tong, J. L. Yeh, S. R. Wang, and B. W. Lee, *Phys. Rev. B* **32**, 8473 (1985).
⁷J. Bohr, R. Feidenhans'l, M. Nielsen, M. Toney, and R. L. Johnson, *Phys. Rev. Lett.* **54**, 1275 (1985).
⁸A. U. MacRae, *Surf. Sci.* **4**, 247 (1966).
⁹I. Hernández-Calderon, H. Höchst, A. Mazur, and J. Pollmann, *J. Vac. Sci. Technol. A* **5**, 2042 (1987).
¹⁰I. Hernández-Calderon and H. Höchst, *Surf. Sci.* **152/153**, 1035 (1985).
¹¹L. Seehofer, I. Krivorotov, and R. L. Johnson, in *Proceedings of the 4th International Conference on the Formation of Semiconductor Interfaces, Jülich, 1993*, edited by B. Lengeler, H. Lüth, W. Mönch, and J. Pollmann (World Scientific, Singapore, 1994), p. 69.; L. Seehofer, Ph.D. thesis, University of Hamburg, 1993.
¹²J. Wever, H. L. Meyerheim, V. Jahns, W. Moritz, and H. Schulz, in *Proceedings of the 4th International Conference on the Formation of Semiconductor Interfaces, Jülich, 1993* (Ref. 11), p. 73.
¹³H. Qu, P. O. Nilsson, J. Kanski, and L. Ilver, *Phys. Rev. B* **39**, 5276 (1989).
¹⁴M. Taniguchi, S. Suga, M. Seki, S. Shin, K. L. I. Kobayashi, and H. Kanzaki, *J. Phys. C* **16**, L45 (1983).
¹⁵H. Höchst and I. Hernández-Calderon, *J. Vac. Sci. Technol. A* **3**, 911 (1985).
¹⁶L. Ö. Olsson, C. B. M. Andersson, M. C. Håkansson, L. Ilver, J. Kanski, and U. O. Karlsson (unpublished).
¹⁷C. B. M. Andersson, U. O. Karlsson, M. C. Håkansson, L. Ö. Olsson, L. Ilver, J. Kanski, P. O. Nilsson, and P. E. S. Persson, *Surf. Sci.* **307–309**, 885 (1994).
¹⁸X. Hou, G. Dong, X. Ding, and X. Wang, *Surf. Sci.* **183**, 123 (1987).
¹⁹M. Nishida, *J. Phys. C* **14**, 535 (1981).
²⁰C. B. M. Andersson, L. Ö. Olsson, M. C. Håkansson, L. Ilver, U. O. Karlsson, and J. Kanski, *J. Phys. (Paris)* (to be published).
²¹Y. W. Mo, *Phys. Rev. Lett.* **71**, 2923 (1993).

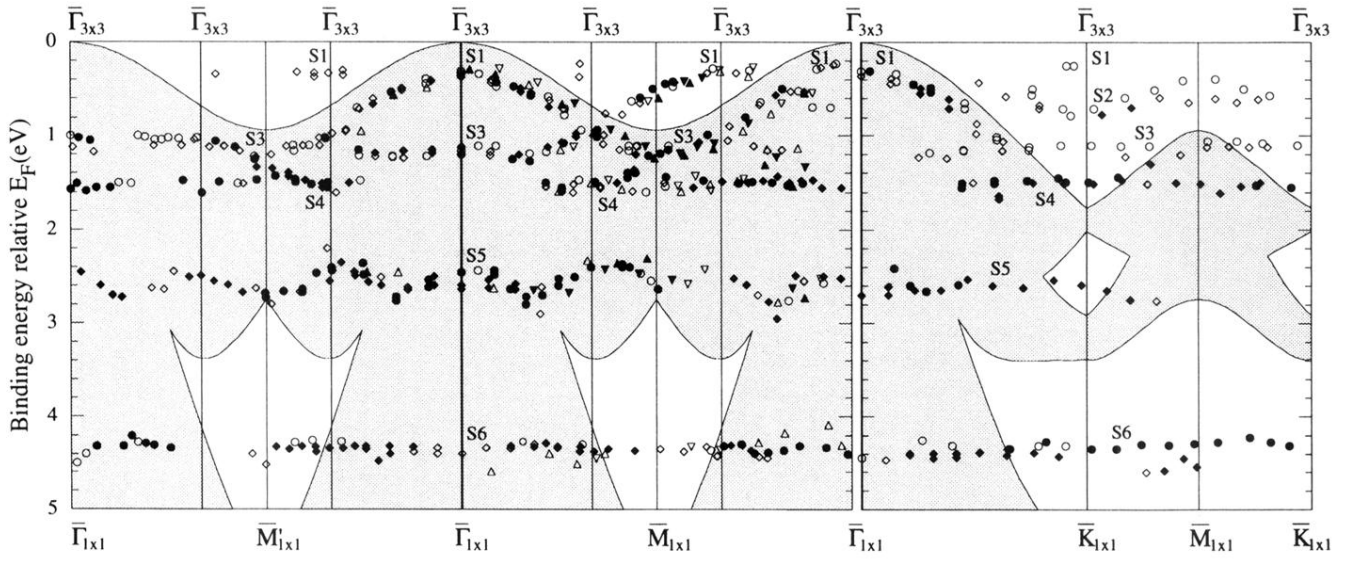


FIG. 2. Structure plot of spectral features that are candidates for being surface induced, obtained at 16.8 eV (\diamond), 20.0 eV (\triangle), 21.2 eV (\circ), and 24.0 eV (∇). Filled symbols represent well-defined structures while open symbols refer to weaker structures. The shaded area is the surface projection of bulk bands. The symmetry points of the 1×1 SBZ and the zone centers of the reconstructed 3×3 SBZ is given, with $\bar{\Gamma}$ corresponding to normal emission marked by a heavy line. The S1 and S3 surface bands are tentatively indicated by lines in regions where DOS structures interfere.

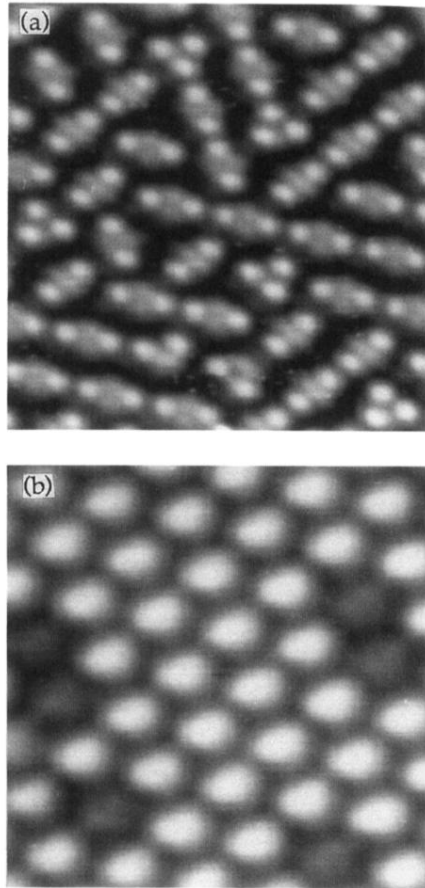


FIG. 6. STM images, $80 \times 80 \text{ \AA}^2$, of the reconstructed 3×3 surface at a tunneling current of 1.4 nA and sample bias of -2.2 V (a) and -0.6 V (b). Two different surface units exist with the high bias image (a) revealing three (β) or four (α) protrusions per unit cell.